

# Single-spin asymmetries for small-angle pion production in high-energy hadron collisions

A. Ahmedov<sup>1,a</sup>, I.V. Akushevich<sup>2,b</sup>, E.A. Kuraev<sup>1,c</sup>, P.G. Ratcliffe<sup>3,4,d</sup>

<sup>1</sup> Joint Inst. for Nuclear Research, 141980 Dubna, Moscow region, Russia

<sup>2</sup> Nat. Center of Particle and High Energy Physics, Bogdanovich Str. 153, 220040 Minsk, Belarus

<sup>3</sup> Dip. di Scienze CC.FF.MM., University degli Studi dell'Insubria, via Lucini 3, 22100 Como, Italia

<sup>4</sup> Ist. Naz. di Fisica Nucleare—sezione di Milano, via Celoria 16, 20133, Milano, Italia

Received: 11 May 1999 / Revised version: 22 July 1999 / Published online: 3 November 1999

**Abstract.** Within the framework of a simple model, we study single-spin asymmetries for pion production in hadron–hadron collisions at high energies with one hadron polarized. The asymmetries are generated via a mechanism of final- (initial-) state interactions. For peripheral kinematics, we find nonzero asymmetries at the high-energy limit when the pion belongs to the fragmentation region of the polarized proton. Numerical results and comparison with existing experimental data are presented. We also discuss the relationship with Odderon exchange phenomenology.

## 1 Introduction

Single-spin correlations have been the subject of theoretical [1–15] and experimental [16–20] study since the seventies. Earlier theoretical work paid attention mainly to time-reversal invariance violation in hadron-scattering processes. No such effect was found, whereas C-odd single-spin correlation asymmetries were observed at the level of  $\sim 10\%$  in SLAC experiments, in which 10–12 GeV electrons and positrons were scattered off polarized protons (with large error bars, however), and later in Fermilab experiments at higher energies. The capabilities of modern CERN and DESY experiments permit the reduction of these errors because of much improved statistics. We argue here that at small momentum transfer, large effects may be understood in the framework of Pomeron and Odderon exchange models and may thus provide an independent method of studying the characteristics of such exchanges in high-energy peripheral hadron scattering.

The appearance of single-spin correlations and associated asymmetries in differential cross sections is due to a quantum effect of interference between real and imaginary parts of different amplitudes. In phenomenological approaches, the amplitudes have been used in a Breit–Wigner form, and the asymmetries turn out to be proportional to the width-to-mass ratio of the resonance [4, 5]. For the case of polarized proton–proton collisions, with the production of pions through some intermediate nucleon resonance state in peripheral kinematics (PK), the

asymmetry may be as large as 20–40% [6]. Another mechanism for the generation of imaginary parts in scattering amplitudes is due to initial- or final-state interactions. In lowest-order perturbation theory, such contributions can arise from the interference between the Born amplitude and one-loop amplitudes with a nonzero  $s$ -channel imaginary part [1].

A similar phenomenon has been found for the case of large-angle production: for the kinematics of large  $p_T$  and large  $x_F$  of the detected hadron, single-spin asymmetries are generated by twist-3 parton correlation functions constructed from quark and gluon fields. For this case, the theoretical approach within the framework of perturbative QCD has been discussed recently by several authors [2, 3, 7, 12, 15].

Here we consider peripheral kinematics: The unpolarized proton produces a jet moving along the initial direction of motion, which is then not detected, whereas the jet produced by the polarized proton contains a detected pion. The asymmetry originates from a term  $i\epsilon^{p_1 p_2 l a} = (i/2)s[\mathbf{l} \wedge \mathbf{a}]_z$ , where  $p_1$  and  $p_2$  are the 4-momenta of the initial protons,  $l$  is the momentum of the pion in the center-of mass-system (CMS) and  $a$  is the spin 4-vector of the proton with momentum  $p_2$ , which is essentially a 2-component vector located in the plane transverse to the beam axis (the  $z$  direction of the initial-state proton with momentum  $p_1$ ), and  $s = 4E^2$  is the square of the total CMS energy.

For high enough energies, the description in terms of Regge trajectories is more convenient, because for small enough momentum transfer, the contribution of operators of all twists will be of the same order of magnitude. Here the even (spin-independent) part of the differential

Correspondence to: <sup>a</sup> ahmedov@sunse.jinr.ru,

<sup>b</sup> aku@hep.by,

<sup>c</sup> kuraev@thsun1.jinr.ru,

<sup>d</sup> pgr@fis.unico.it

cross section is determined by Pomeron exchange, whereas the spin-dependent part, arising from interference between one- and two-gluon exchange amplitudes, should be described by the Odderon trajectory. Note that quark exchange in the  $t$ -channel only gives a small contribution, suppressed by a factor of  $m^2/s$ , where  $m$  is the proton mass. Thus, the study of single-spin asymmetries in PK may provide information on the Odderon intercept. In this paper, using a QED-like framework with point-like hadrons, we calculate the asymmetry, defined as follows:

$$A = \frac{d\sigma(a, l) - d\sigma(-a, l)}{d\sigma(a, l) + d\sigma(-a, l)} = \alpha_{\text{QED}} \frac{(\mathbf{a} \wedge \mathbf{l})_z}{m} \mathcal{A}(r, x), \quad (1)$$

in which  $\alpha_{\text{QED}} = 1/137$  is the QED coupling constant, and the resolving power,  $\mathcal{A}(r, x)$ , is a function of  $r = l_{\perp}/m$  (the transverse momentum of pion in units of the proton mass,  $m$ ) and  $x = 2l_0/\sqrt{s}$  (its energy fraction,  $x \sim \mathcal{O}(1)$ ). We shall show that  $\mathcal{A}(r, x)$  is a smooth rising function of  $x$  of order unity. Thus, naively replacing the QED coupling constant by that of QCD or by that of the Pomeron or Odderon coupling with the proton, we find that the asymmetry may be large for large enough values of  $l_{\perp}$ ; this is in qualitative agreement with experimental data [16–18, 20].

We should recall before proceeding that although the diagrams considered (see Fig. 1) would be excluded by naive color conservation in purely perturbative QCD, they represent precisely the two-gluon exchange topology generally held responsible for the Pomeron contribution, e.g., to the total cross section [21, 22].

The paper is organized as follows. In Sect. 2, we calculate the expressions for the squared matrix elements summed over spin states for processes of neutral- and charged-pion production in the framework of our QED-like approach. The corresponding charge-odd interferences for these channels are considered in Sect. 3, in which we first obtain the expressions for asymmetries in an exclusive setup (when both the nucleon and pion from the jet developing along the direction of polarized proton are fixed in the experiment); we then estimate the ratio of odd and even parts of the cross section averaged over final proton momenta. In the conclusion, we discuss the situation in which a hadron is detected in the opposite direction, and we also discuss the role of higher-order perturbation theory contributions and their relationship to Odderon exchange.

## 2 Calculation of the cross section

Consider first the process

$$P(p_1) + P(p_2) \rightarrow P(p'_1) + P(p'_2) + \pi_0(l), \quad (2)$$

for which the relevant Born-approximation diagrams are shown in Fig. 1. We use the Sudakov expansion for the

momenta of the problem, introducing the almost light-like vectors

$$\begin{aligned} \tilde{p}_1^\mu &= p_1^\mu - \frac{m^2}{s} p_2^\mu, \\ \tilde{p}_2^\mu &= p_2^\mu - \frac{m^2}{s} p_1^\mu. \end{aligned} \quad (3)$$

With these we define the following parametrization of the momenta in the problem:

$$\begin{aligned} q^\mu &= p_1^\mu - p'_1{}^\mu = \alpha \tilde{p}_2^\mu + \beta \tilde{p}_1^\mu + q_\perp^\mu, \\ p'_2{}^\mu &= (1-x) \tilde{p}_2^\mu + \beta' \tilde{p}_1^\mu + p_\perp^\mu, \\ l^\mu &= x \tilde{p}_2^\mu + \beta_l \tilde{p}_1^\mu + l_\perp^\mu, \\ q_\perp^\mu &= p_\perp^\mu + l_\perp^\mu. \end{aligned} \quad (4)$$

The transverse parts,  $v_\perp$ , obey

$$\begin{aligned} v_\perp \cdot p_1 &= 0 = v_\perp \cdot p_2, \\ v_\perp^2 &= -\mathbf{v}^2 < 0. \end{aligned} \quad (5)$$

We have also used the specific properties of PK: The sum of pion and proton energy fractions from the jet moving along initial polarized proton is equal to unity,  $x \sim \mathcal{O}(1)$ ; moreover, the reality conditions for final particles permit the neglect of the “small” components of the momenta:

$$s\beta' = \frac{m^2 + \mathbf{p}_2^2}{1-x}, \quad (6)$$

$$s\beta_l = \frac{\mathbf{l}^2}{x}. \quad (7)$$

Here and in what follows, we neglect the pion mass squared compared to that of the proton. The intermediate fermion denominators in the Born graphs (see Fig. 1) are then given by

$$d_1 = k_1^2 - m^2 \simeq \frac{m^2 x^2 + (x\mathbf{q} - \mathbf{l})^2}{x(1-x)}, \quad (8)$$

$$d_2 = k_2^2 - m^2 \simeq -\frac{m^2 x^2 + \mathbf{l}^2}{x}. \quad (9)$$

Note that  $k_1^2$  is just the invariant mass squared of the jet moving along  $\mathbf{p}_2$ . We shall show that the dominant contribution arises when this quantity is of the order of some nucleon mass squared.

In the Born approximation, the matrix element has the following form:

$$\mathcal{M}_{\pi^0} = \frac{4\pi\alpha g}{q^2} J_\mu^{(1)}(p_1) D^{\mu\nu}(q) J_\nu^{(2)}(p_2), \quad (10)$$

where  $\alpha = \alpha_{\text{QED}}$ ,  $g$  is the pion–nucleon coupling constant and  $D^{\mu\nu}$  is the exchange photon polarization tensor. The current vectors introduced are

$$\begin{aligned} J_\mu^{(1)}(p_1) &= \bar{u}(p'_1) \gamma_\mu u(p_1), \\ J_\nu^{(2)}(p_2) &= \bar{u}(p'_2) O_\nu u(p_2), \end{aligned} \quad (11)$$

Single-Spin Asymmetries . . .

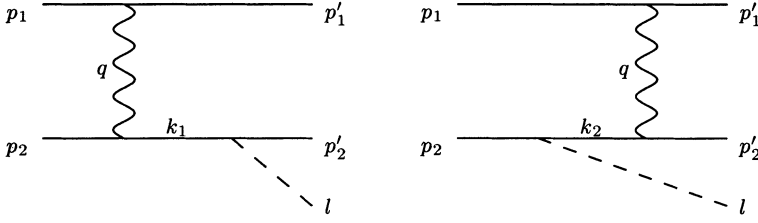


**Fig. 1.** The amplitudes for the process  $pp \rightarrow pp\pi$  in the Born approximation; the proton with momentum  $p_2$  is polarized

where

$$\begin{aligned} O_\nu &= \frac{1}{d_1} \gamma_5 (\not{p}'_2 + \not{l} + m) \gamma_\nu + \frac{1}{d_2} \gamma_\nu (\not{p}_2 - \not{l} + m) \gamma_5 \\ &= \gamma_5 \left[ \frac{\not{l} \gamma_\nu}{d_1} - \frac{\gamma_\nu \not{l}}{d_2} \right]. \end{aligned} \quad (12)$$

In the last step of (12), we have used the Dirac equation for free protons. For PK, only the so-called nonsense components of the decomposition of the photon polarization tensor give a nonvanishing contribution in the high-energy limit:

$$\begin{aligned} D^{\mu\nu} &= g_\perp^{\mu\nu} + 2(p_1^\mu p_2^\nu + p_1^\nu p_2^\mu)/s \\ &\simeq 2p_1^\mu p_2^\nu/s. \end{aligned} \quad (13)$$

Further simplifications may be made by the use of the current conservation condition,  $q \cdot J^{(2)} = 0$ , which implies  $p_1 \cdot J^{(2)} \simeq -q_\perp \cdot J^{(2)}/\beta$ .

As a result, the matrix element in the Born approximation becomes

$$\mathcal{M}_{\pi^0} = -\frac{8\pi\alpha g}{\beta s q^2} \bar{u}(p'_1) \not{p}_2 u(p_1) \bar{u}(p'_2) O u(p_2), \quad (14)$$

where  $O = q'_\perp O_\nu$ . Here the exchange denominator is  $q^2 = -(\mathbf{q}^2 + q_m^2)$ , with  $q_m^2 = m^2(\tilde{s}/s)^2$  and  $\tilde{s} = (m^2 x + \mathbf{p}_2^2)/(1-x) + \mathbf{l}^2/x$ . However, in order to regulate the infrared divergences, we shall use a massive vector-particle propagator:  $q^2 = -(\mathbf{q}^2 + \mu^2)$ . For the modulus squared of the Born matrix element, summed over spin states, we thus obtain

$$\sum_{\text{spins}} |\mathcal{M}_{\pi^0}|^2 = (16\pi g \alpha)^2 \frac{s^2 x^2 \mathbf{q}^2}{d_1 (-d_2) (\mathbf{q}^2 + \mu^2)^2}. \quad (15)$$

Note that here we consider the hadrons as point-like particles, and so the high-frequency contributions are not negligible (unrealistically so). Thus, although all integrals are in fact convergent, we now introduce a form factor of the form  $\exp(-\mathbf{q}^2/q_c^2)$ , with  $q_c \sim 1 \text{ GeV}$ , the effect of varying  $q_c$  will be shown later.

As is well known, single-spin correlation effects are absent in the Born approximation, as a consequence of the reality of Born amplitudes and the form of the proton spin-density matrix:

$$\begin{aligned} u(p_2, a) \bar{u}(p_2, a) &= (\not{p}_2 + m)(1 + \gamma_5 \not{a}), \\ \text{tr}[\gamma_5 \not{a} \not{b} \not{c} \not{d}] &= 4i\epsilon^{abcd}. \end{aligned} \quad (16)$$

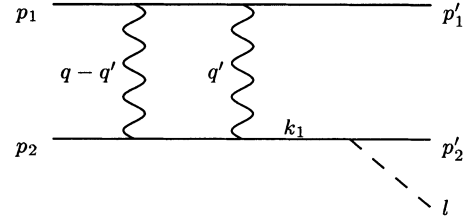


**Fig. 2.** An example higher-order contribution to the process  $pp \rightarrow pp\pi$ , as considered in the text

It is also well known that in the case of elastic small-angle charged-particle scattering, the Born amplitude acquires a Coulomb phase factor,  $\exp[i\alpha\pi \ln(-q^2/\mu^2)]$ , when multiphoton exchange is taken into account. A similar factor appears in the case of inelastic processes in PK, such as those we are considering here.

### 3 Calculation of the spin dependence

For the spin-dependent part of the interference between single- and double-photon exchange amplitudes (see Fig. 2), a calculation similar to that performed above gives

$$\begin{aligned} \sum_{\text{spins}} \Delta |\mathcal{M}_{\pi^0}|^2 &= \frac{2^{11} \pi^2 \alpha^3 g^2 s}{\tilde{s}^2 |\mathbf{q}|^4} \ln \left( \frac{|\mathbf{q}|^2}{\mu^2} \right) \\ &\times \frac{i}{4} \text{tr}[-\gamma_5 \not{a} \tilde{O} (\not{p}'_2 + m) O (\not{p}'_2 + m) \not{p}_1 (\not{p}_2 + m)], \end{aligned} \quad (17)$$

in which again,  $O = q'_\perp O_\nu$ . After calculating the trace we obtain, for the exclusive setup,

$$\begin{aligned} A &= \frac{\Delta \sum |\mathcal{M}_{\pi^0}|^2}{\sum |\mathcal{M}_{\pi^0}|^2} \\ &= 4\alpha \ln(\mathbf{q}^2/\mu^2) m |\mathbf{a}| |\mathbf{q}| \sin \phi_q \\ &\times \frac{[x\tilde{s} - 2\mathbf{q} \cdot \mathbf{l}][x\mathbf{q}^2 + (1-x)2\mathbf{q} \cdot \mathbf{l}]}{\tilde{s} d_2 \mathbf{q}^2}, \end{aligned} \quad (18)$$

where  $\phi_q$  is the azimuthal angle between the transverse 2-vectors  $\mathbf{a}$  and  $\mathbf{q}$ . We note that the asymmetry is finite in the small- $\mathbf{q}$  limit.

The differential cross section in the Born approximation is

$$\frac{d\sigma_B}{dx dr} = \frac{2\alpha_{\text{QED}} \alpha_{pp\pi}}{m^2} \frac{r}{x(1+\rho)^2} \left[ \ln \frac{(1+\rho)^2}{\sigma} - 1 \right], \quad (19)$$

where  $\alpha_{pp\pi} = g^2/(4\pi) \approx 3$ ,  $\rho = r^2/x^2$  and  $\sigma = (\mu^2 + q_m^2)/M^2$ . The Born cross section is a monotonically rising function of  $x$  ( $\sim x^3$ ) for small  $x$ . It falls rapidly as  $1/l^3$  for large pion transverse momentum  $\mathbf{l}$  and reaches the maximum value for  $l_\perp \sim mx/\sqrt{3}$ . The asymmetry in the inclusive setup, defined as a ratio of even and odd parts of the cross section averaged over transverse momenta, may be written, for small  $\sigma$ , in the form:

$$A = \frac{\int d^2\mathbf{q} \sum \Delta|M|^2}{\int d^2\mathbf{q} \sum |M|^2} = |\mathbf{a}| \sin \phi_l \frac{4\alpha_{\text{QED}}R}{r \left[ \ln \frac{(1+\rho)^2}{\sigma} - 1 \right]}, \quad (20)$$

with

$$R = x \ln(1+\rho) \ln \frac{1+\rho}{\sigma} + x(1-x) \times \left[ \frac{\rho}{2(1+\rho)} \ln^2 \sigma + f_1(\rho, x) \ln \sigma + f_2(\rho, x) \right], \quad (21)$$

in which  $f_{1,2}$  are rather flat functions; the complete expression for  $R$  is given in the appendix. The results of a numerical calculation of the asymmetry in the inclusive setup as a function of  $x$  for various values of the form-factor cutoff  $q_c$  and as a function of  $\mathbf{l}$  for a various values of the Feynman variable  $x$  are presented in Fig. 3. Note that in Fig. 3a, the experimental values of  $l_\perp$  vary with  $x_F$  [17]; thus our theoretical curves are calculated for the same set of values; the mean  $l_\perp$  varies between 0.4 and 1.2 GeV. While the detailed dependence on  $x$  and  $l_\perp$  is not entirely reproduced, the general trends are seen to be correct.

A similar calculation for the case of  $\pi^+$  production in the small- $\mathbf{q}$  limit yields

$$\begin{aligned} x^2 \sum |\mathcal{M}_{\pi^+}|^2 &= (1-x)^2 \sum |\mathcal{M}_{\pi^0}|^2, \\ x^2 \sum \Delta|\mathcal{M}_{\pi^+}|^2 &= (1-x)^2 \sum \Delta|\mathcal{M}_{\pi^0}|^2, \end{aligned} \quad (22)$$

where  $\sum \Delta|\mathcal{M}|^2$  stands for the spin-weighted sum. Thus, the asymmetries for  $\pi^+$  production roughly coincide with those for the  $\pi^0$  case.

## 4 Conclusions

We see that asymmetry effects due to single transverse polarization are not suppressed in the limit of large total CMS energy  $\sqrt{s}$ , in the case in which the produced hadron belongs to the jet of the polarized proton.

The overall normalization depends on the detailed mechanism of vector-meson (photon, Pomeron or gluon) interaction with nucleons and is bound to the choice of the parameters  $\alpha$  and  $\mu$ . In inclusive measurements, when the momentum of the pion is measured and the jets escape detection for relatively large  $t$  (but  $-t \ll s$ ), the interference between graphs with one and two exchange gluons (in the same color state) will dominate. In the case

in which protons are in the final state, it is natural then to interpret the exchange as a Pomeron (leading-order interference terms) or an Odderon (higher-order interference terms). In both of these cases, the asymmetry is expected to be of the same order and to have the same (qualitative) dependence on  $x_F$  and transverse momentum. However, the overall normalization factor will change, so we consider it as a fitting parameter. Thus, the naive replacements  $\alpha \rightarrow \alpha_s$  and  $\mu \rightarrow \Lambda_{\text{QCD}}$  lead to asymmetries of the same order as those found experimentally and which grow with transverse momentum for small values.

Numerical analysis shows that the model constructed agrees qualitatively with the existing data for  $\pi^+$  and  $\pi^0$  [17, 18, 16, 20]. The overall normalization factor is  $\sim 25$ –35, which, when multiplied by a generalized coupling constant equaling  $\alpha_{\text{QED}}$ , is equivalent to an overall normalization factor of  $\sim 0.3$ . The asymmetry for  $\pi^-$  also can be considered within this scheme; however,  $2 \rightarrow 4$  processes have to be considered instead of  $2 \rightarrow 3$ . In this case, the role of intermediate  $\Delta$  resonances would also have to be evaluated carefully. This subject, as well as a more exact description of  $\pi^{+,0}$  cases, will be investigated elsewhere.

It should be noted that in the case in which the pion is detected in the direction of the jet moving in the opposite direction (i.e., along  $\mathbf{p}_1$ ) the asymmetry effect will be suppressed in the  $s \rightarrow \infty$  limit. In fact, information on the transverse polarization of proton  $p_2$  cannot be transmitted to jet components developing from proton  $p_1$  unless at least one “sense” component of the virtual photon polarization tensor is used,  $g_{11}^{\mu\nu}$ ; consequently, it will be suppressed by powers of  $m^2/s$ .<sup>1</sup>

In particular, for elastic proton–proton scattering, when an unpolarized scattered proton with momentum  $p'_1$  is detected, we obtain:

$$A_{p(p'_1)} = \alpha \frac{5m\mathbf{q}^2(\mathbf{a} \wedge \mathbf{q})_z}{2s^2}. \quad (23)$$

Higher-order QCD effects may be taken into account by the introduction of a factor  $(s/s_0)^{a_O}$  into the odd part of the elastic proton–proton-scattering zero-angle amplitude, where  $a_O$  is the Odderon intercept. Thus, the asymmetry considered here, associated with twice the imaginary part, acquires a factor  $a_O^2(s/s_0)^{a_O - a_P}$ , where  $a_P$  is the Pomeron intercept. Given that  $a_O < a_P$ , such a factor will eventually suppress the asymmetry in the ultrahigh-energy limit<sup>2</sup>. However, our interest lies in the lower-energy region, accessible experimentally at present. Moreover, the lack of knowledge on the precise value of  $a_O$  leaves the entire question of asymptotics uncertain. Finally, we note that for small-angle scattering of electrons off polarized protons, the Odderon contribution manifests itself in higher orders of perturbation theory because of the conversion of photons into gluons through the  $\gamma\gamma \rightarrow gg$  and  $\gamma g \rightarrow gg$  kernels; this may also be investigated at DESY.

<sup>1</sup> We are grateful to Lev N. Lipatov for discussions on this point.

<sup>2</sup> We are grateful to Sergey Troshin for bringing this point to our attention.

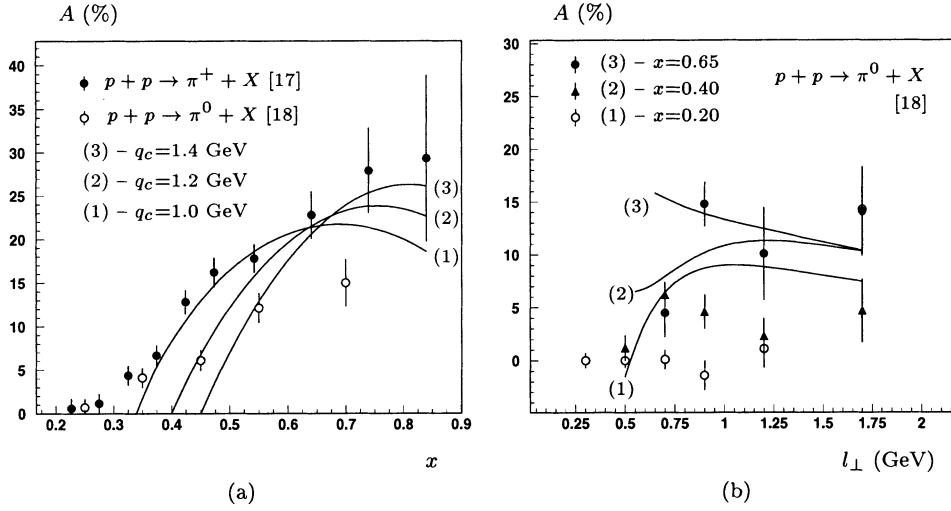


**Fig. 3.** The model calculations for the asymmetry plotted as a function of **a**  $x$  (with  $l_{\perp}$  varying point-by-point as explained in the text) for various values of the form-factor cutoff,  $q_c$ , and **b**  $l_{\perp}$  for various values of  $x$

*Acknowledgements.* One of us (E.A.K.) is grateful to Pierre Gauron, Basarab Nicolescu and Gregory P. Korchemsky for useful discussions. We are also grateful to the Cariplo Foundation for Scientific Research, for financial support, and the Dip. di Scienze CC.FF.MM., Università degli Studi dell'Insubria, sede di Como, for its hospitality while this work was performed.

## Appendix

After some simple operations, the odd part of the cross section, averaged over  $\mathbf{q}$ , may be put into the following form:

$$\begin{aligned} & \int \frac{d^2\mathbf{q}}{\pi} \sum \Delta |M|^2 \\ &= \frac{2^{10}(\pi g)^2 \alpha_{\text{QED}}^3 x s^2}{d_2^2} \frac{|\mathbf{a}| \sin \phi_l}{r} \\ & \times \int \frac{d^2\mathbf{q}}{\pi} \frac{\ln(\mathbf{q}^2/\mu^2) \mathbf{q} \cdot \mathbf{l}}{(\mathbf{q}^2 + \mu^2)^2 d_1 \tilde{s}} \\ & \times [x^2 \mathbf{q}^2 \tilde{s} - 4(\mathbf{q} \cdot \mathbf{l})^2 - 2x d_2 \mathbf{q} \cdot \mathbf{l}], \quad (24) \end{aligned}$$

where we have used another equivalent form of the numerator in (18):

$$\begin{aligned} & [x\tilde{s} - 2\mathbf{q} \cdot \mathbf{l}] [x\mathbf{q}^2 + (1-x)2\mathbf{q} \cdot \mathbf{l}] \\ &= x^2 \mathbf{q}^2 \tilde{s} - 4(\mathbf{q} \cdot \mathbf{l})^2 - 2x d_2 \mathbf{q} \cdot \mathbf{l}. \quad (25) \end{aligned}$$

We write the integrals of the three terms in square brackets in (24) as  $J_{1,2,3}$ , respectively. The quantity  $R$  introduced in (21) may then be reexpressed in terms of the  $J_i$ :

$$R = \frac{\sum_{i=1}^3 J_i}{x(1-x)}. \quad (26)$$

For the first term, we have

$$J_1 = x(1-x) \int \frac{d^2\mathbf{q}}{\pi} \mathbf{q} \cdot \mathbf{l}$$

$$\frac{\ln(1/\sigma) + \ln(\mathbf{q}^2/m^2)}{\mathbf{q}^2(\mathbf{q}^2 - 2\mathbf{q} \cdot \mathbf{l}/x + (1+\rho)m^2)}, \quad (27)$$

where  $\rho = \mathbf{l}^2/(m^2 x^2)$ . Using the Feynman trick of combining the denominators, we adopt the following representation for the logarithm:

$$\left(\frac{m^2}{\mathbf{q}^2}\right) \ln\left(\frac{\mathbf{q}^2}{m^2}\right) = -\frac{d}{dg} \left(\frac{\mathbf{q}^2}{m^2}\right)^{-g} \Bigg|_{g=1}.$$

The denominators may be combined by the use of the identity

$$\frac{1}{u^g v^h} = \frac{\Gamma(g+h)}{\Gamma(g)\Gamma(h)} \int_0^1 dz \frac{(1-z)^{g-1} z^{h-1}}{[(1-z)u + zv]^{g+h}}. \quad (28)$$

The further standard procedure of performing the  $d^2\mathbf{q}$  integration and subsequent differentiation with respect to  $g$  and integration over  $z$  yields

$$J_1 = x^2(1-x) \ln(1+\rho) \ln \frac{1+\rho}{\sigma}. \quad (29)$$

In the evaluation of  $J_2$ , we may set  $\sigma = 0$  in the denominator. Joining the first two denominators, we have

$$\frac{1}{d_1 \tilde{s}} = \frac{(1-x)^2}{x} \int_0^1 dy [\mathbf{q}^2 - 2\mathbf{q} \cdot \mathbf{l} \frac{\eta}{x} + \eta m^2(1+\rho)]^{-2}, \quad (30)$$

where  $\eta = x+y(1-x)$ . Then, following a procedure similar to that given above, we obtain

$$\begin{aligned} J_2 = & -4[x(1-x)\rho]^2 \int_0^1 dy \eta \int_0^1 dz z^2(1-z) \\ & \times \left[ \frac{\rho \eta^2 z^2}{D^3} (2L-1) + \frac{3L}{2D^2} \right], \quad (31) \end{aligned}$$

where  $L = \ln(D/(1-z)\sigma)$  and  $D = \eta(1+\rho)z - \eta^2 z^2 \rho + (1-z)\sigma$ . We note that we may set  $\sigma = 0$  in the expression

for  $D$ , although in evaluating  $J_3$ , we cannot omit  $\sigma$  in the denominator. Nevertheless, using the identity

$$\ln\left(\frac{\mathbf{q}^2}{\sigma m^2}\right) = \ln\left(\frac{\mathbf{q}^2/m^2 + \sigma}{\sigma}\right) - \ln\left(1 + \frac{\sigma m^2}{\mathbf{q}^2}\right), \quad (32)$$

we may apply the procedure of differentiation to the first term. The second is important in the region  $\mathbf{q}^2 \sim \sigma m^2$  and may be evaluated explicitly:

$$\begin{aligned} & -2x^2(1+\rho) \int \frac{d^2\mathbf{q}}{\pi} (\mathbf{q} \cdot \mathbf{l})^2 \frac{\ln(1 + \frac{\sigma m^2}{\mathbf{q}^2})}{(\mathbf{q}^2/m^2 + \sigma)^2 d_1 \bar{s}} \\ &= -\frac{x^2(1-x)^2 \rho}{1+\rho} \int_0^\infty \frac{dz z \ln(1 + \frac{1}{z})}{(1+z)^2} \\ &= -\frac{x^2(1-x)^2 \rho}{1+\rho} \left(\frac{\pi^2}{6} - 1\right). \end{aligned} \quad (33)$$

The total answer for  $J_3$  is then

$$\begin{aligned} J_3 &= -\frac{x^2(1-x)^2 \rho}{1+\rho} \left(\frac{\pi^2}{6} - 1\right) \\ &+ 2x^3(1-x)^2 \rho(1+\rho) \int_0^1 dy \int_0^1 dz z(1-z) \\ &\times \left[ \frac{\rho z^2 \eta^2 (2L-1)}{D^3} + \frac{L}{2D^2} \right]. \end{aligned} \quad (34)$$

## References

1. G.L. Kane, J. Pumplin, W. Repko, Phys. Rev. Lett. **41**, 1689 (1978)
2. J. Qiu, G. Sterman, Phys. Rev. Lett. **67**, 2264 (1991)
3. J. Qiu, G. Sterman, Nucl. Phys. B **378**, 52 (1992)
4. R. Barni, G. Preparata, P.G. Ratcliffe, Phys. Lett. B **296**, 251 (1992)
5. P.G. Ratcliffe, in Proceedings of the X Int. Symp. on High Energy Spin Physics, Nagoya, Nov. 1992, edited by T. Hasegawa, N. Horikawa, A. Masaike, S. Sawada (University Acad. Press, 1993), p. 635
6. A. Arbuzov, et al., Phys. Atom. Nucl. **57**, 1004 (1994)
7. A.V. Efremov, V.M. Korotkiyan, O.V. Teryaev, Phys. Lett. B **348**, 577 (1995)
8. V.M. Korotkiian, O.V. Teryaev, Phys. Rev. D **52**, 4775 (1995)
9. M. Anselmino, M. Boglione, F. Murgia, Phys. Lett. B **362**, 164 (1995)
10. M. Anselmino, E. Leader, F. Murgia, Phys. Rev. D **56**, 6021 (1997)
11. N. Hammon, O. Teryaev, A. Schäfer, Phys. Lett. B **390**, 409 (1997)
12. J. Qiu, G. Sterman, Phys. Rev. D **59**, 014004 (1999)
13. M. Anselmino, F. Murgia, Phys. Lett. B **442**, 470 (1998)
14. N. Hammon, B. Ehrnsperger, A. Schäfer, J. Phys. G **24**, 991 (1998)
15. P.G. Ratcliffe, Eur. Phys. J. C **8**, 403 (1999)
16. D.L. Adams, et al., FNAL-E581 Collaboration, Phys. Lett. B **261**, 201 (1991)
17. D.L. Adams, et al., FNAL-E704 Collaboration, Phys. Lett. B **264**, 462 (1991)
18. D.L. Adams, et al., FNAL-E581 Collaboration, Z. Phys. C **56**, 181 (1992)
19. A. Bravar, et al., FNAL-E704 Collaboration, Phys. Rev. Lett. **75**, 3073 (1995)
20. D.L. Adams, et al., FNAL-E704 Collaboration, Nucl. Phys. B **510**, 3 (1998)
21. F.E. Low, Phys. Rev. D **12**, 163 (1975)
22. S. Nussinov, Phys. Rev. Lett. **34**, 1286 (1975)